P 1981-4

81_01

Time, Frequency, and z-Domain Modified Nodal Analysis of Switched-Capacitor Networks

JOOS VANDEWALLE, MEMBER, IEEE, HUGO J. DE MAN, AND JAN RABAEY

Abstract—A rigorous and general derivation of the modified nodal equations needed for a time, frequency and z-domain analysis of multiphase switched-capacitor networks is given. Also a general equivalent circuit for switched-capacitor networks is derived. This technique allows to handle continuous coupling, piecewise-constant inputs as well as continuous inputs. These results can be used to adapt existing circuit analysis programs, based on modified nodal analysis, for efficient simulation of switched-capacitor networks.

Manuscript received November 12, 1979; revised September 5, 1980.
The authors are with the Katholieke Universiteit Leuven, Heverlee, Belgium.

I. Introduction

RECENTLY much attention has been devoted to switched-capacitor networks (SC networks). A topic of major concern is the construction of simple, efficient, and general simulation programs for such networks. One particular successful approach [1] in this direction is the adaptation of the modified nodal analysis [2] to SC networks. It requires only minor modifications of existing programs based on MNA in order to analyze SC networks efficiently. Here we describe a unifying framework for this time-domain approach and for approaches based on z-

0098-4094/81/0300-0186$00.75 ©1981 IEEE

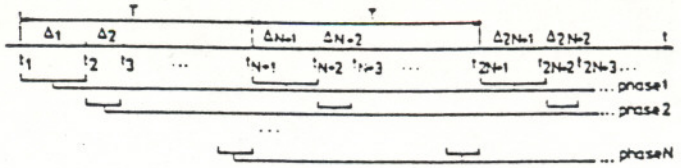


Fig. 1. The timing instances and phases of an N-phase SC network.

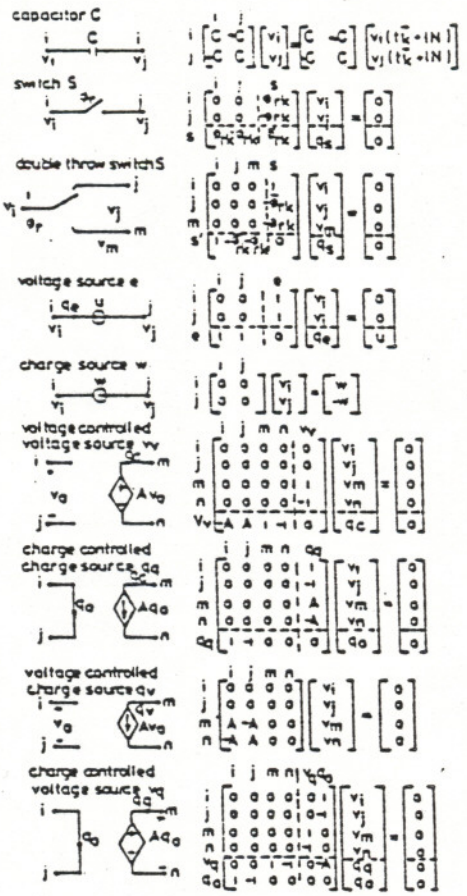


Fig. 2. Contribution or "stamp" for the different components of a SC network to the MNA equations (1).

transforms. This will provide additional insight in the system-theoretic aspects of SC networks. It turns out that there exists an easily computable z-domain transfer matrix which completely characterizes the signal handling capabilities from the N phases at the input to the N phases at the output. Many of our results can be obtained by adapting [3]–[7], [9], [10] to the MNA framework and to multiphase SC networks. However we prefer the direct derivation because of its conceptual simplicity and the direct link with the computer implementation.

II. Time-Domain MNA

We consider arbitrary linear networks containing ideal switches, capacitors, independent voltage and charge sources (VS and QS), and four types of dependent sources (VCVS, QCVS, VCQS, QCQS). The switches are controlled by Boolean clock variables $\phi_i(t)=0$, or 1. $\phi_i(t)=0$ (resp., $\phi_i(t)=1$) corresponds to an open (resp., closed) switch at time t if this switch is driven by clock i.

The time is partitioned into time slots $\Delta_m=(t_m, t_{m+1}]$ such that the clock signals (and hence the network) do not vary in Δ_m. We assume that the clock signals are T-periodic, i.e., $\phi_i(t+lT)=\phi_i(t)\ \forall t, i$ (Fig. 1). Each period has N time slots. The union of the time slots $\Delta_k, \Delta_{k+N}, \Delta_{k+2N}, \cdots$ is called phase k. All time slots of phase k have the same duration and the clock values are the same, i.e., $\phi_i(t)=\phi_{ik}$, for all t in phase k. We also assume that there are no resistors in the networks. Hence, there are no transients in the waveforms. In practice this is not a severe restriction since all SC networks are designed to reach their equilibrium state quickly enough otherwise their operation would be unreliable.

In Theorem 1 we show how the time-domain equations of a SC network can be set up in the MNA framework [2]. It is useful to keep in mind that MNA is an extension of the nodal equations by adding some branch relations and that each component contributes a pattern (called stamp) given in Fig. 2 to the equation (1).

Theorem 1: The above defined linear T-periodic switched capacitor network is described in the time domain by the equations for $t \in \Delta_{k+lN}$

$$\left[\begin{array}{c|c} A_k & B_k \\ \hline C_k & D_k \end{array}\right]\left[\begin{array}{c} v(t) \\ \hline q(t) \end{array}\right] = \left[\begin{array}{c} E_k v(t_{k+lN}^-) \\ \hline 0 \end{array}\right] + \left[\begin{array}{c} w(t) \\ \hline u(t) \end{array}\right] \quad (1)$$

where $v(t)$ (resp., $u(t)$) is the vector of the voltage responses at the nodes (resp., voltage sources in some selected branches) and where $q(t)$ (resp., $w(t)$) is the vector of the charges transferred in some selected branches (resp., injected by charge sources in the nodes) between t_{k+lN}^- and t for $t \in \Delta_{k+lN}$ and where the contributions to A_k, B_k, C_k, D_k, E_k, $w(t)$, and $u(t)$ are constructed as follows.

Construction of the Time Domain MNA Equations (1)

1) Choose the unknown variables of the network as follows. The voltages at all the nodes (except the reference voltage) constitute the unknown voltage vector $v(t)$. The charges in switches, voltage sources, the controlled branches of VCVS, QCQS, and QCVS's, and controlling branches of QCQS's constitute the unknown charge vector $q(t)$. The voltage input $u(t)$ (resp., charge input $w(t)$) has the same size as $q(t)$ (resp., $v(t)$).

2) Set up (1) with A_k, B_k, C_k, D_k, E_k, $u(t)$, and $w(t)$ zero.

3) For each component of the circuit identify the stamp of Fig. 2. Observe that the stamp of a switch includes the Boolean variable of the clock which controls the switch. If the component is connected to the reference node delete the corresponding row and column in the stamp. Using the indexes of the rows and columns in the stamp add the contribution to the appropriate entries in the matrices A_k, B_k, C_k, D_k of the left-hand side of (1), and to E_k, $u(t)$, and $w(t)$ of the right-hand side of (1).

Proof: The charge $w(t)$ injected in the nodes between t_{k+ln}^- and $t \in \Delta_{k+ln}$ is equal to the net charge flowing away from this node in the other branches or using Fig. 2:

$$A_k v(t) - E_k v(t_{k+lN}^-) + B_k q(t) = w(t). \quad (2)$$

The remainder equations of (1) are precisely a vector formulation of the constitutive equations in some selected branches. □

Clearly equations of (1) can be set up easily by computer using the stamps and compare favorably with the involved topologic or numerical procedures of [3]–[5], [7], [9], [10]. Other issues are compared in Section V. These equations can be easily extended to include nonperiodic networks and nonlinear voltage controlled capacitors and voltage sources [1]. However the subsequent derivations depend on linearity and periodicity and hence we have assumed these throughout.

Observe that the matrices $A_k = E_k$ and do not depend on k since all stamps of Fig. 2 satisfy this property. In Section V we will see that other stamps which do not satisfy this property are often more efficient. There we discuss also the improvement such stamps can bring to the above construction. The following corollary gives a justification from (1) that the voltage transfer in a SC network is not affected, by a relative change in all capacitor values.

Corollary 1: By multiplying all capacitances and all controlling factors of VCQS by α and by multiplying all controlling factors of QCVS by $1/\alpha$, all charges of a SC network are multiplied by α and all voltages remain unchanged.

Proof: This corollary follows directly from (1). □

In order to solve (1) we decompose the input signals and the output signals into piecewise-constant contributions and the remainder waveforms and obtain the following result.

Theorem 2: The above defined linear T-periodic SC network is described in the time domain by

$$\left[\begin{array}{c|c} A_k & B_k \\ \hline C_k & D_k \end{array}\right]\left[\begin{array}{c} v_{k+lN} \\ \hline q_{k+lN} \end{array}\right] = \left[\begin{array}{c} E_k v_{k+lN-1} \\ \hline 0 \end{array}\right] + \left[\begin{array}{c} w_{k+lN} \\ \hline u_{k+lN} \end{array}\right] \quad (3.a)$$

and

$$\left[\begin{array}{c|c} A_k & B_k \\ \hline C_k & D_k \end{array}\right]\left[\begin{array}{c} v^*(t) \\ \hline q^*(t) \end{array}\right] = \left[\begin{array}{c} w^*(t) \\ \hline u^*(t) \end{array}\right], \qquad \text{for } t \in \Delta_{k+lN} \quad (3.b)$$

where

$$v_{k+lN} \triangleq v(t_{k+lN+1}^-) \quad (4.a)$$

$$v^*(t) \triangleq v(t) - v_{k+lN}, \qquad \text{for } t \in \Delta_{kl+N} \quad (4.b)$$

and analogous decompositions for $q(t)$, $w(t)$, and $u(t)$.

Proof: Substitute (4) in (1) and evaluate it at $t = t_{k+lN+1}^-$ in order to obtain (3.a). Subtracting (3.a) from (1) generates (3.b). Conversely adding (3.a) and (3.b) and substituting (4) gives (1). □

In words the Theorem 2 says the following. Decompose the signals into a piecewise-constant waveform such that the amplitude in each time slot is equal to the value at the end of this time slot and a remainder waveform. The output is then the sum of a piecewise-constant waveform obtained by solving the N-periodic implicit linear algebraic and difference equation (3.a) and a remainder output obtained by solving the linear algebraic equations (3.b) (capacitive feedthrough).

Roughly speaking the existence and uniqueness of the solutions of (3) is guaranteed for almost all networks of interest. For passive networks there are even topologic conditions. In the case that the independent voltage and charge sources are the only active components, it can be shown that (3) is always *solvable* if in *time* slot k there is *no cut set* of charge sources and open switches and *no loop* of voltage sources and closed switches. This topological condition is trivially satisfied by any practical circuit since this condition is either violated if the excitation is unacceptable or if one of the switches can be reversed in this time slot.

III. z-Domain MNA

In this section we use z-transform techniques to solve (3). We make again use of the linearity of the capacitors and the controlled sources. Since (3) is time-varying the techniques of the z-transform are not readily applicable. Fortunately (3) is *periodic* and hence we can adapt a method of Jury [6, p. 57]. We partition the sequence of values at the end of each time slot $v_1, v_2, v_3, v_{N-1}, v_N, v_{N+1}\cdots$ into N different sequences each having the same phase: $v_1, v_{N+1}, v_{2N+1}, \cdots$ and $v_2, v_{N+2}, v_{2N+2}, \cdots$, etc., until $v_N, v_{2N}, v_{3N}, \cdots$ (Fig. 1). We take the standard z-transform of these N sequences.

$$V_k(z) \triangleq \mathcal{Z}\{v_{k+lN}\} = \sum_{l=0}^{\infty} v_{k+lN} z^{-l} \tag{5}$$

where $k=1,2,\cdots,N$. Analogously we obtain $Q_k(z)$, $W_k(z)$, and $U_k(z)$. Remember also [6] that if $v_i=0$, $i<0$

$$\mathcal{Z}\{v_{k+(l-1)N}\} = z^{-1}V_k(z). \tag{6}$$

Theorem 3: The above described linear T-periodic SC network is described in the z-domain by

$$\left[\begin{array}{cccc:cccc} A_1 & & & -E_1z^{-1} & B_1 & & & \\ -E_2 & A_2 & & & & B_2 & & \\ & -E_3 & A_3 & & & & B_3 & \\ & & \ddots & \ddots & & & & \ddots \\ & & -E_N & A_N & & & & B_N \\ \hdashline C_1 & & & & D_1 & & & \\ & C_2 & & & & D_2 & & \\ & & C_3 & & & & D_3 & \\ & & & \ddots & & & & \ddots \\ & & & C_N & & & & D_N \end{array}\right] \left[\begin{array}{c} V_1 \\ V_2 \\ V_3 \\ \cdots \\ V_N \\ \hdashline Q_1 \\ Q_2 \\ Q_3 \\ \cdots \\ Q_N \end{array}\right] = \left[\begin{array}{c} W_1 \\ W_2 \\ W_3 \\ \cdots \\ W_N \\ \hdashline U_1 \\ U_2 \\ U_3 \\ \cdots \\ U_N \end{array}\right] \tag{7}$$

where the missing entries are zero.

Proof: By writing (3.a) in full for $k=1,2,\cdots,N$ we obtain an augmented set of time-invariant algebraic and difference equations on which (5), (6) can be applied in order to obtain (7). □

As an interesting alternative to solving (3.a) in the time domain, one can equivalently solve the z-domain equations (7). In terms of the inverse of the matrix in (7), which is called the *z-domain transfer matrix*, the equations will become

$$\left[\begin{array}{c} V_1 \\ V_2 \\ \cdots \\ V_N \\ \hdashline Q_1 \\ Q_2 \\ \cdots \\ Q_N \end{array}\right] = \left[\begin{array}{cccc:cccc} G_{11} & G_{12} & \cdots & G_{1N} & H_{11} & H_{12} & \cdots & H_{1N} \\ G_{21} & G_{22} & \cdots & G_{2N} & H_{21} & H_{22} & \cdots & H_{2N} \\ \cdots & \cdots & & \cdots & \cdots & \cdots & & \cdots \\ G_{N1} & G_{N2} & \cdots & G_{NN} & H_{N1} & H_{N2} & \cdots & H_{NN} \\ \hdashline K_{11} & K_{12} & \cdots & K_{1N} & L_{11} & L_{12} & \cdots & L_{1N} \\ K_{21} & K_{22} & \cdots & K_{2N} & L_{21} & L_{22} & \cdots & L_{2N} \\ \cdots & \cdots & & \cdots & \cdots & \cdots & & \cdots \\ K_{N1} & K_{N2} & \cdots & K_{NN} & L_{N1} & L_{N2} & \cdots & L_{NN} \end{array}\right] \left[\begin{array}{c} W_1 \\ W_2 \\ \cdots \\ W_N \\ \hdashline U_1 \\ U_2 \\ \cdots \\ U_N \end{array}\right]. \tag{8}$$

The submatrices G_{kn}, H_{kn}, K_{kn}, L_{kn} allow a very simple interpretation. Up to this point we consider the SC network as a discrete device which transforms the input sequences of samples at t_i^-, $i=1,2,\cdots$ of the voltage sources and charge sources into the output sequences of samples of voltages or charges at t_i^-, $i=1,2,\cdots$. If only nonzero voltages sources are applied during time slots $n, n+N, n+2N,\cdots$ and if the output node voltages are only observed during time slots $k, k+N, k+2N,\cdots$ then $H_{kn}(z)$ relates the z-transform of this input sequence to this output sequence, i.e., $V_k(z)=H_{kn}(z)U_n(z)$ or it relates inputs at phase n to outputs at phase k. In other words $H_{kn}(z)$ is the z-transform of $h_{kn}(mT)$, $m=0,1,\cdots$, i.e., the node voltage responses observed during time slots $k, k+N, k+2N,\cdots$ to unit input voltages applied during time slot n. Clearly $H_{in}(z)$ is the z-transform of the node voltage response during time slots $i, i+N, i+2N,\cdots$ to the same input, and can thus be derived from the same network analyses as $H_{kn}(z)$. Thus one column of the transfer matrix of (8) can be determined from one network analysis.

Corollary 2: Any above defined SC network is completely characterized by the z-domain transfer matrix of (8).

Proof: Observe that the inverse of the matrix of (3.b) can be easily obtained from the z-domain transfer matrix (8) at $z=\infty$:

$$\left[\begin{array}{c} v^*(t) \\ \hdashline q^*(t) \end{array}\right] = \left[\begin{array}{c:c} G_{kk}(\infty) & H_{kk}(\infty) \\ \hdashline K_{kk}(\infty) & L_{kk}(\infty) \end{array}\right] \left[\begin{array}{c} w^*(t) \\ \hdashline u^*(t) \end{array}\right], \quad \text{for } t \in \Delta_{k+lN}. \tag{9}$$

□

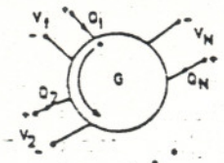


Fig. 3. The symbol of a generalized circulator (6) with constant G.

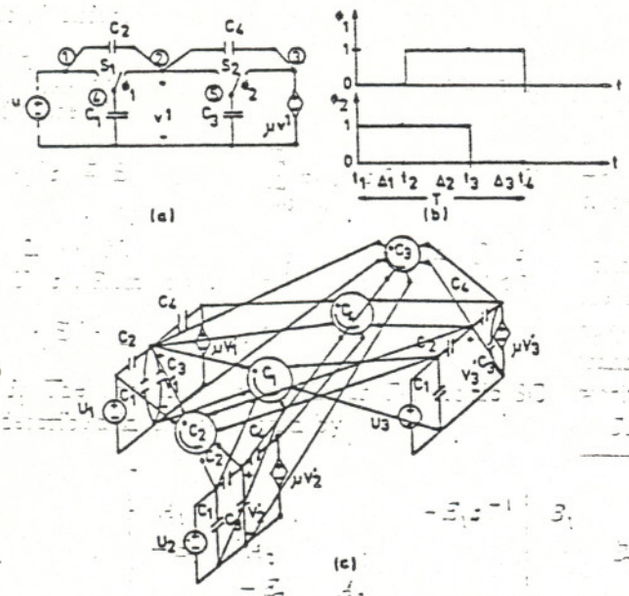


Fig. 4. The SC network of (a) with clock signals (b) has an equivalent circuit (c).

One can wonder next whether there exists a time-invariant network of impedances which is described by (7) and whether such a network can be derived immediately from the SC network. The key idea in obtaining such an equivalent network is to convert the N phases of any branch into N different branches. This converts the different instances of *time* into different locations in *space*. We need the following intrinsic N-port called a *generalized circulator with constant G* which is defined by (Fig. 3)

$$\begin{bmatrix} Q_1 \\ Q_2 \\ Q_3 \\ \cdots \\ Q_N \end{bmatrix} = \begin{bmatrix} 0 & & & & -Gz^{-1} \\ -G & 0 & & & \\ & -G & 0 & \ddots & \\ & & \ddots & \ddots & \\ & & & -G & 0 \end{bmatrix} \begin{bmatrix} V_1 \\ V_2 \\ \cdots \\ V_N \end{bmatrix} \tag{10}$$

Construction of the Equivalent Circuit $\mathcal{N}_e$ of a SC Network $\mathcal{N}$

1) For each of the N phases (i.e., N time slots in one period) a network is drawn with the switches in the correct position for this time slot.

2) The N networks are interconnected by generalized circulators as follows. For each capacitor C_i in the original circuit we need a circulator with constant C_i. Port 1 of this circulator is connected to the corresponding capacitor of the first circuit, port 2 to that of the second circuit and so on. Repeat for each capacitor.

It is easy to check that the resulting network is described by (7). For 2-phase SC networks this equivalent circuit reduces to those of [4], [7] via some transformations (the generalized circulator corresponds to the gyrator of the link two port of [4]). We have applied this algorithm to the circuit of Fig. 4(a) with clock signals of Fig. 4(b) and obtain the equivalent circuit of Fig 4(c).

IV. Frequency-Domain Analysis using MNA

We describe in this section how the practically useful frequency properties can be derived from the time-domain or z-domain analysis of the previous sections. In many applications such as in filtering one is mainly interested in the frequency components of the input and output voltage waveforms. So we will only derive the expressions for voltages. Since a SC network is a time-varying network in general many frequencies appear at the output for a sinusoidal excitation.

Theorem 4: The above described linear T-periodic SC-network generates for a voltage excitation $u(t)$ with Fourier transform $U(\omega)$ a voltage response $v(t)$ with Fourier transform $V(\omega)$ given by

$$V(\omega) = \sum_{n=-\infty}^{+\infty} X(\omega, \omega - n\omega_s) U(\omega - n\omega_s); \tag{11}$$

The Fourier transform $\hat{V}_k(\omega)$ of $\hat{v}_k(t)$ which is the voltage $v(t)$ observed during phase k and zero outside is

$$\hat{V}_k(\omega) = \sum_{n=-\infty}^{+\infty} X_k(\omega, \omega - n\omega_s) U(\omega - n\omega_s) \tag{12}$$

where $\omega_s = 2\pi/T$ and *the transmission function*

$$X(\omega, \Omega) = \sum_{k=1}^{N} X_k(\omega, \Omega)$$

with the *transmission function* $X_k(\omega, \Omega)$ of phase k given by

$$X_k(\omega, \Omega) = \alpha_k(\omega) e^{-j\omega t_{k+1}} \sum_{l=1}^{N} e^{j\Omega t_{l+1}} H_{kl}(e^{j\Omega T}) + \left[\alpha_k(\omega - \Omega) - \alpha_k(\omega)\right] \exp\left[j(\Omega - \omega) t_{k+1}\right] H_{kk}(\infty) \tag{13}$$

with H_{kl} defined by (8) and

$$\alpha_k(\rho) \triangleq 2\{\sin[\rho(t_{k+1} - t_k)/2] \cdot \exp[j\rho(t_{k+1} - t_k)/2]\}/T\rho. \tag{14}$$

Proof: The derivation of (11) is done by first calculating the Fourier transform of the piecewise-constant contribution $\tilde{v}_k(t)$ in $\hat{v}_k(t)$ using (8) and $\hat{V}_k(\omega)$ using Theorem 2 and then summing over all phases $k = 1, 2, \cdots, N$. The response is first calculated for a sinusoidal excitation and afterwards extended to arbitrary excitation. The details are given in the Appendix. □

Clearly the first term in (13) takes into account the piecewise-constant signals and the second term the continuous coupling. From (11), (12) it follows that a sinusoidal input $u(t)$ generates an output which has a line spectrum whose lines are ω_s a part. Mostly one is only interested in the contribution at the same frequency as the input. This is among others the case if the bandwidth of

$u(t)$ is smaller than half the sampling frequency. For such cases we define the following practical *frequency-domain transfer functions* $H(\omega)$ (resp., $H_k(\omega)$) [5]. Apply a sinusoidal excitation $u(t)=Ue^{j\omega t}$ and compute or measure the frequency component at the same pulsation ω in the output $v(t)$ (resp., $v_k(t)$), then $H(\omega)$ (resp., $H_k(\omega)$) relates the phasor U to that of the output $v(t)$ (resp., $\hat{v}_k(t)$) at pulsation ω. Theorem 4 allows to compute H and H_k easily.

Corollary 3: Under the assumptions of Theorem 4

$$H_k(\omega)=\alpha_k(\omega)e^{-j\omega t_{k-1}}\sum_{l=1}^{N}e^{j\omega t_{l-1}}H_{kl}(e^{j\omega T}) + \left[\frac{t_{k+1}-t_k}{T}-\alpha_k(\omega)\right]H_{kk}(\infty) \tag{15}$$

$$H(\omega)=\sum_{k=1}^{N}H_k(\omega) \tag{16}$$

where α_k is given by (14).

Proof: Take only the term with $n=0$ in the sum (11) and (12). □

V. Example and Computational Aspects

In this section we first illustrate the above derivations on our example of Fig. 4. Then we discuss the computer implementations via time domain analysis (3.a) and via the z-domain analysis (7) and compare both briefly with other techniques [3]–[5], [7], [9], [10]. The analysis via the time domain has been implemented in the DIANA-program and is further described in [1].

The matrices of the basic time-domain equations (3.a) for the circuit of Fig. 4(a) are obtained using the construction given in section I ($A_k=E_k$)

$$\left[\begin{array}{c|c} A_k & B_k \\ \hline C_k & D_k \end{array}\right] = \begin{array}{c} \\ 1 \\ 2 \\ 3 \\ 4 \\ 5 \\ \hline S_1 \\ S_2 \\ V_o \\ U \end{array} \begin{array}{c} \begin{array}{ccccc} 1 & 2 & 3 & 4 & 5 \end{array} \\ \left[\begin{array}{ccccc|ccccc} C_2 & -C_2 & 0 & 0 & 0 & -\phi_{1k} & 0 & 0 & 1 \\ -C_2 & C_2+C_4 & -C_4 & 0 & 0 & -\bar{\phi}_{1k} & -\phi_{2k} & 0 & 0 \\ 0 & -C_4 & C_4 & 0 & 0 & 0 & -\bar{\phi}_{2k} & 1 & 0 \\ 0 & 0 & 0 & C_1 & 0 & 1 & 0 & 0 & 0 \\ 0 & 0 & 0 & 0 & C_3 & 0 & 1 & 0 & 0 \\ \hline -\phi_{1k} & -\bar{\phi}_{1k} & 0 & 1 & 0 & 0 & 0 & 0 & 0 \\ 0 & -\phi_{2k} & -\bar{\phi}_{2k} & 0 & 1 & 0 & 0 & 0 & 0 \\ 0 & -\mu & 1 & 0 & 0 & 0 & 0 & 0 & 0 \\ 1 & 0 & 0 & 0 & 0 & 0 & 0 & 0 & 0 \end{array}\right] \end{array}$$

$$\left[\begin{array}{c} w_{k+1N} \\ \hline u_{k+1N} \end{array}\right] = \left[\begin{array}{c} 0 \\ 0 \\ 0 \\ 0 \\ 0 \\ \hline 0 \\ 0 \\ 0 \\ u_{k+1N} \end{array}\right]. \tag{17}$$

These equations are equivalent with the time-domain equations for the multiphase SC networks via topological [5], [10] or numerical [9] procedures. The number of equations in [5], [9], [10] may, however, be smaller. This corresponds to a preliminary elimination of some variables. Clearly any SC network analysis approach in the time domain must be equivalent with our MNA equations (3.a) the same way as for networks without switches [2]. Some straightforward eliminations can, without any complication, be included in our approach by using a macromodel, which we call a *composite branch*. A frequently used composite branch is that of the subnetwork of Fig. 5. By using the basic derivation it would need a 5×5 matrix and as variables v_i, v_j, v_m, v_l, and q_S. If node l is not connected to any other branch and if one is not interested in v_l and q_S this subnetwork has a stamp:

$$\begin{array}{c} \\ i \\ j \\ m \end{array} \begin{array}{c} \begin{array}{ccc} i & j & m \end{array} \\ \left[\begin{array}{ccc} C & -C\bar{\phi}_k & -C\phi_k \\ -C\bar{\phi}_k & C\bar{\phi}_k & 0 \\ -C\phi_k & 0 & C\phi_k \end{array}\right] \end{array} \left[\begin{array}{c} v_i \\ v_j \\ v_m \end{array}\right]$$

$$= \begin{array}{c} \begin{array}{ccc} i & j & m \end{array} \\ \left[\begin{array}{ccc} C & -C\bar{\phi}_{k-1} & -C\phi_{k-1} \\ -C\bar{\phi}_k & C\bar{\phi}_k\bar{\phi}_{k-1} & C\bar{\phi}_k\phi_{k-1} \\ -C\phi_k & C\phi_k\bar{\phi}_{k-1} & C\phi_k\phi_{k-1} \end{array}\right] \end{array} \left[\begin{array}{c} v_i(t_{k+1N}) \\ v_j(t_{k+1N}) \\ v_m(t_{k+1N}) \end{array}\right]. \tag{18}$$

Using the stamps of such composite branches the construction of the time-domain equations can be rephrased.



Fig. 5. A useful composite branch.

There are less unknown variables, since no internal node voltages of a composite branch appear and since some branch charges are eliminated. In our case we only have 5 equations

$$\begin{array}{c} \\ 1 \\ 2 \\ 3 \\ V_o \\ U \end{array} \begin{array}{c} \begin{array}{ccccc} 1 & 2 & 3 & V_o & U \end{array} \\ \left[\begin{array}{ccc:cc} C_1\phi_{1k}+C_2 & -C_2 & 0 & 0 & 1 \\ -C_2 & C_1\bar{\phi}_{1k}+C_2+C_3\phi_{2k}+C_4 & -C_4 & 0 & 0 \\ 0 & -C_4 & C_3\bar{\phi}_{2k}+C_4 & 1 & 0 \\ \hdashline 0 & -\mu & 1 & 0 & 0 \\ 1 & 0 & 0 & 0 & 0 \end{array}\right] \end{array} \begin{bmatrix} v_{1k+lN} \\ v_{2k+lN} \\ v_{3k+lN} \\ \hdashline q_{ck+lN} \\ q_{Ek+lN} \end{bmatrix}$$

$$= \left[\begin{array}{ccc} C_1\phi_{1k}\phi_{1k-1}+C_2 & C_1\phi_{1k}\bar{\phi}_{1k-1}-C_2 & 0 \\ C_1\bar{\phi}_{1k}\phi_{1k-1}-C_2 & C_2\bar{\phi}_{1k}\bar{\phi}_{1k-1}+C_2+C_3\phi_{2k}\phi_{2k-1}+C_4 & C_3\phi_{2k}\bar{\phi}_{2k-1}-C_4 \\ 0 & C_3\bar{\phi}_{2k}\phi_{2k-1}-C_4 & C_3\bar{\phi}_{2k}\bar{\phi}_{2k-1}+C_4 \\ \hdashline 0 & 0 & 0 \\ 0 & 0 & 0 \end{array}\right] \begin{bmatrix} v_{1k-1+lN} \\ v_{2k-1+lN} \\ v_{3k-1+lN} \end{bmatrix} + \begin{bmatrix} 0 \\ 0 \\ 0 \\ \hdashline 0 \\ u_{k+lN} \end{bmatrix}. \quad (19)$$

Observe that with composite branches the matrices A_k and E_k for the N phases and the left- and right-hand side of (3a) can be different. Experience has shown that the use of some simple composite branches leads to sets of equations of the same sizes comparable to those of [5], [9], [10]. The equations in the z-domain have a size 3 times that of (19) since there are 3 phases.

$$\left[\begin{array}{ccc:ccc:ccc:cc:cc:cc} C_2 & 0 & -C_2 & -z^{-1}C_2 & z^{-1}C_2 & 0 & 0 & 1 & & & & \\ -C_2 & C_1+C_2+C_3+C_4 & -C_4 & z^{-1}(C_2-C_1) & -z^{-1}(C_2+C_4) & z^{-1}(C_4-C_3) & 0 & 0 & 0 & 0 & 0 & \\ 0 & -C_4 & C_4 & 0 & z^{-1}C_4 & -z^{-1}C_4 & 1 & 0 & & & & \\ \hdashline -C_2 & -C_1+C_2 & 0 & C_1+C_2 & -C_2 & 0 & & & 0 & 1 & & \\ C_2 & -C_2-C_3-C_4 & C_4 & -C_2 & C_2+C_3+C_4 & -C_4 & 0 & & 0 & 0 & 0 & \\ 0 & C_4 & -C_4 & 0 & -C_4 & C_4 & & & 1 & 0 & & \\ \hdashline & & & -C_1-C_2 & C_2 & 0 & C_1+C_2 & -C_2 & 0 & & 0 & 1 \\ & 0 & & C_2 & -C_2-C_4 & C_4 & -C_2 & C_2+C_4 & -C_4 & 0 & 0 & 0 \\ & & & 0 & -C_3+C_4 & -C_4 & 0 & -C_4 & C_3+C_4 & & 1 & 0 \\ \hdashline 0 & -\mu & 1 & & 0 & & & 0 & & 0 & 0 & 0 \\ 1 & 0 & 0 & & & & & & & & & \\ \hdashline & & & 0 & -\mu & 1 & & & & & & \\ & 0 & & 1 & 0 & 0 & & 0 & & 0 & 0 & 0 \\ \hdashline & & & & & & 0 & -\mu & 1 & & & \\ & 0 & & & 0 & & 1 & 0 & 0 & 0 & 0 & 0 \end{array}\right]$$

$$\begin{bmatrix} V_{11} \\ V_{21} \\ V_{31} \\ \hdashline V_{12} \\ V_{22} \\ V_{32} \\ \hdashline V_{13} \\ V_{23} \\ V_{33} \\ \hdashline Q_{11} \\ Q_{21} \\ \hdashline Q_{12} \\ Q_{22} \\ \hdashline Q_{13} \\ Q_{23} \end{bmatrix} = \begin{bmatrix} 0 \\ 0 \\ 0 \\ \hdashline 0 \\ 0 \\ 0 \\ \hdashline 0 \\ 0 \\ 0 \\ \hdashline 0 \\ U_1 \\ \hdashline 0 \\ U_2 \\ \hdashline 0 \\ U_3 \end{bmatrix}. \quad (20)$$

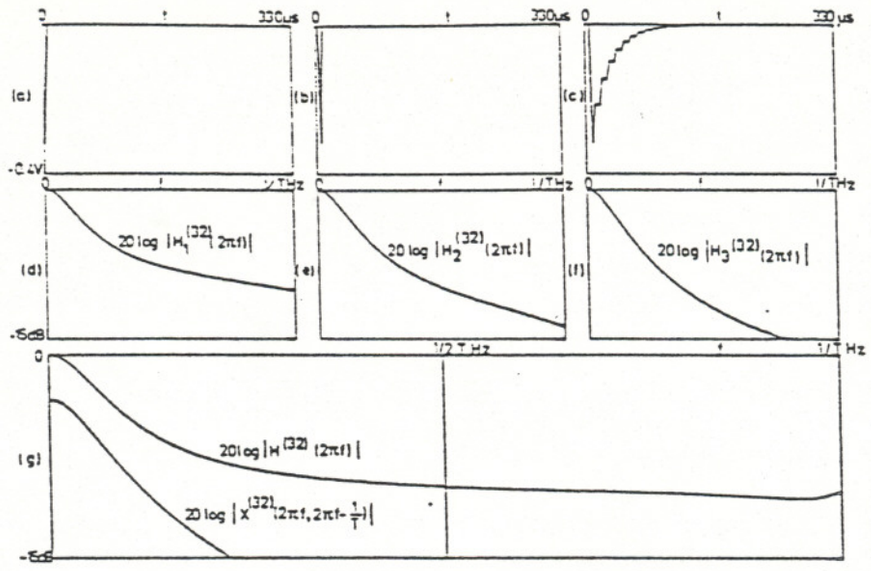


Fig. 6. Computer analysis results of the SC network of Fig. 1. (a)–(c) Responses on impulses in phase 1, 2 and 3. (d)–(e) Frequency-domain transfer functions $H_k^{(32)}(\omega)$ of phases $k=1$, 2, and 3. (f) Frequency-domain transfer function $H^{(32)}(\omega)$ and aliasing term $X^{(32)}(\omega, \omega-(2\pi/T))$.

The z-domain transfer matrix is the inverse of the matrix in (20) and is not included for brevity. The frequency-domain characteristics $X_k(\omega, \Omega)$ (aliasing effects and frequency-domain transfer function $H_k(\omega)$) can then be derived easily from (13)–(16). Usually one is only interested in the input–output relationship. In our example the relation between u (branch 3) and v_3 (node 3) is desired. Hence we need the entries $H_{kl}^{(32)}(z)$ with $k, l=1,2,3$ which relate U_1, U_2, U_3 to V_{31}, V_{32}, and V_{33}. These can be combined in (13) to obtain $X_k^{(32)}(\omega, \Omega)$ with $k=1,2,3$.

The practical computer implementation of the time and frequency responses is now briefly described, and applied on our example.

Computation of the Piecewise-Constant Response to a Piecewise-Constant Voltage Excitation $u_{j1}, u_{j2}, u_{j3}, \cdots$ in Branch j

1) Set up the equations (3a) and use as many composite branches as possible.

2) For each phase reorder the equations and find the LU decomposition (see [2]).

3) Start with zero initial conditions and solve (3a) with sparse matrix techniques for time slot $1,2,3,\cdots$. Each time the right-hand side of (3a) is obtained from the previous time slot.

This procedure is implemented as an option in the DIANA program. It generates for the circuit of Fig. 4 the responses given in Fig. 6(a, b, c) on impulses in phase 1, 2, and 3, respectively.

Computation of $X_k^{(i,j)}(\omega, \Omega)$ or $H_k^{(i,j)}(\omega)$ $k=1,\cdots,N$ via the Time Domain (3.a)

1) Apply a unit voltage excitation in branch j during phase $k=1,2,\cdots,N$ and compute for each k the piecewise-constant voltage response $\mathcal{K}_k^{(ij)}$ at the node i as described above.

2) Decompose each $\mathcal{K}_k^{(ij)}$ into N signals $h_{kl}^{(ij)}(mT)$ and apply the discrete Fourier transform on these N^2 signals in order to obtain $H_{kl}^{(ij)}(e^{j\Omega T})$ for $k, l=1,2,\cdots,N$.

3) Combine the results as in (13) or (16). Remember from the z-transform [6] that

$$H_{kk}^{(ij)}(\infty)=h_{kk}^{(ij)}(0). \tag{21}$$

Observe here that the number of resonses to be computed in [1] can be reduced using the adjoint SC network [8] if only one value of k is of interest. By applying this approach on our example of Fig. 4 we obtain the plots for the frequency-domain transfer function and the aliasing effect as given in Fig. 6.

Computation of $X_k^{(i,j)}(\omega, \Omega)$ $k=1,2,\cdots,N$ via the z-Domain (7)

1) Set up the equation (7) using the stamps.

2) For each value of Ω of interest set $z=e^{j\Omega T}$ and $U_{jl}=e^{j\Omega t_{l-1}}$, $l=1,2,\cdots,N$ and all other inputs zero. Solve (7) for these values using sparse matrix techniques in order to obtain

$$\sum_{l=1}^{N} e^{j\Omega t_{l-1}} H_{kl}^{(ij)}(e^{j\Omega T}), \qquad \text{for } k=1,2,\cdots,N.$$

3) Solve (7) for $z=\infty$, $U_{jl}=\delta_{kl}$ with $l=1,2,\cdots,N$. Combine the results as in (13) or (15).

Let us now compare the two techniques. Clearly (3a) is an N times smaller set of equations than (7) but it has to be solved more often. Also the time-domain technique requires some FFT's which can be time consuming and can be inaccurate for very selective filters. On the other hand, the time-domain technique allows a mixed mode simulation of SC circuits along with the digital control circuitry as implemented in DIANA [1], [11].

Moreover, it allows a study of the nonideal effects of

SC circuits: offset and leakage current drift, nonlinear distortion, and clock feedthrough [1], [11].

The computations presented in [3]–[5], [7], [9], [10] all use the z-domain approach and in some form or another require to solve sets of equations equivalent to (7). Some efficiency can be obtained by making use of the structure of the problem in [5], [9]. It is however believed that the formulation (7) allows a clear view on all issues involved in using the z-domain technique. Further ideas in this direction are currently being investigated.

Concerning other useful design characteristics of SC (e.g., noise performance, sensitivity, group delay) we just mention here that the adjoint SC network allows [8] computational savings which are even more impressive than for *RLC* circuits.

V. Conclusions

It is shown that the widely used MNA technique can be easily adapted to analyze SC networks. It provides us also with a general equivalent circuit and additional insight in the signal handling capabilities of SC networks. The z-domain transfer matrix turns out to be a key tool in obtaining frequency characteristics and is in fact a hybrid matrix of the equivalent circuit. Two practical computations of these frequency characteristics are derived from the results. One is based on a repeated solution of (3a) in the time domain and its implementation in DIANA has allowed to analyze successfully many SC circuits [1], [11]. The other is based on the solution of (7) for suitable excitations and seems to be computationally even more attractive.

Appendix
Proof of Theorem 4

We calculate first the spectrum of the response for a sinusoidal excitation $u(t)=Ue^{j\Omega t}$. Let $v_k(t)$ be the response sampled at the end of the time slots $\Delta_k, \Delta_{k+N}, \cdots$. Remember that $H_{kl}(z)$ is the z-transform of $h_{kl}(mT)$, $m=0,1,\cdots$, then we have in general from (8) for this sinusoidal excitation

$$\tilde{v}_k(t)=\sum_{n=-\infty}^{+\infty}\delta(t-nT-t_{k+1})\cdot\left[\sum_{l=1}^{N}\left(\sum_{m=0}^{\infty}h_{kl}(mT)Ue^{j\Omega[(n-m)T+t_{l+1}]}\right)\right]$$
$$=\left(\sum_{n=-\infty}^{+\infty}\delta(t-nT-t_{k+1})e^{j\Omega nT}\right)\left(\sum_{l=1}^{N}e^{j\Omega t_{l+1}}H_{kl}(e^{j\Omega T})U\right). \quad (A.1)$$

The Fourier transform of this sinusoidally modulated pulse train is

$$\tilde{V}_k(\omega)=\sum_{n=-\infty}^{+\infty}\omega_s\delta(\omega-\Omega-n\omega_s)\cdot\sum_{l=1}^{N}e^{j(\Omega t_{l+1}-\omega t_{k+1})}H_{kl}(e^{j\Omega T})U \quad (A.2)$$

which has only contributions at the pulsations $\omega=\Omega+n\omega_s$.

In order to derive $\hat{V}_k(\omega)$ we define a block waveform $s_k(t)$ which is 1 in Δ_k and zero outside. Using Theorem 2 and (9) we have

$$\hat{v}_k(t)=\sum_{l=-\infty}^{+\infty}s_{k+lN}(t)v(t)$$
$$=\sum_{l=-\infty}^{+\infty}s_{k+lN}(t)v_{k+lN}+\sum_{l=-\infty}^{+\infty}s_{k+lN}(t)v^*(t)$$
$$=\tilde{v}_k(t)*r_k(t)+H_{kk}(\infty)U\cdot\sum_{l=-\infty}^{+\infty}s_{k+lN}(t)(e^{j\Omega T}-e^{j\Omega t_{k+lN+1}}) \quad (A.3)$$

where $r_k(t)=1$ for $t_k-t_{k+1}<t\leq 0$. From (A.2) we have for the first term of the right-hand side of (A.3):

$$\mathcal{F}\{v_k(t)*r_k(t)\}=2\pi\alpha_k(\omega)\sum_{l=1}^{N}H_{kl}(e^{j\Omega T})\cdot e^{j(\Omega t_{l+1}-\omega t_{k+1})}\cdot\sum_{n=-\infty}^{+\infty}\delta(\omega-\Omega-n\omega_s). \quad (A.4)$$

The Fourier transform of the second term in (A.3) can be obtained by standard techniques as

$$\mathcal{F}\left\{\sum_{l=-\infty}^{+\infty}e^{j\Omega t}s_{k+lN}(t)\right\}=2\pi\alpha_k(\omega-\Omega)e^{j(\Omega-\omega)t_{k+1}}\sum_{n=-\infty}^{+\infty}\delta(\omega-\Omega-n\omega_s) \quad (A.5)$$

and

$$\mathcal{F}\left\{\sum_{l=-\infty}^{+\infty}s_{k+lN}(t)e^{j\Omega t_{k+lN+1}}\right\}=2\pi\alpha_k(\omega)e^{j(\Omega-\omega)t_{k+1}}\sum_{n=-\infty}^{+\infty}\delta(\omega-\Omega-n\omega_s). \quad (A.6)$$

This implies that the spectrum $\hat{V}_k(\omega)$ for the sinusoidal excitation $u(t)=Ue^{j\Omega t}$ is

$$\hat{V}_k(\omega)=X_k(\omega,\Omega)U2\pi\sum_{n=-\infty}^{+\infty}\delta(\omega-\Omega-n\omega_s). \quad (A.7)$$

The linearity of the SC network then implies that the response to an arbitrary input

$$u(t)=\frac{1}{2\pi}\int_{-\infty}^{+\infty}U(\Omega)e^{j\Omega t}\,d\Omega$$

has a spectrum

$$\hat{V}_k(\omega)=\int_{-\infty}^{+\infty}X_k(\omega,\Omega)U(\Omega)\sum_{n=-\infty}^{+\infty}\delta(\omega-\Omega-n\omega_s)\,d\Omega.$$

This implies (12). □

Acknowledgment

The authors appreciate the improvements suggested by L. Claesen and the reviewers and the interesting discussions with Y. P. Tsividis and F. Brglez.

REFERENCES

[1] H. De Man, J. Rabaey, G. Arnout, and J. Vandewalle, "Practical implementation of a general computer aided design technique for switched capacitor circuits," *IEEE J. Solid-State Circuits*, vol. SC-15, pp. 190–200, Apr. 1980.

[2] C-W. Ho, A. Ruehli, and P. Brennan, "The modified nodal approach to network analysis," *IEEE Trans. Circuits Syst.*, vol. CAS-22, pp. 504–509, June 1975.

[3] M. L. Liou and Y. L. Kuo, "Exact analysis of switched capacitor circuits with arbitrary inputs," *IEEE Trans. Circuits Syst.*, vol. CAS-26, pp. 213–223, April 1979.

[4] C. F. Kurth and G. S. Moschytz, "Two-port analysis of switched-capacitor network using four-port equivalent circuits in the z-domain," *IEEE Trans. Circuits Syst.*, vol. CAS-26, pp. 166–180, Mar. 1979.

[5] Y. P. Tsividis, "Analysis of switched capacitive networks," *IEEE Trans. Circuits Syst.*, vol. CAS-26, pp. 935–947, Nov. 1979.

[6] E. I. Jury, *Theory and Application of the z-Transform Method*. New York: Wiley, 1964.

[7] Y. L. Kuo, M. L. Liou, and J. W. Kasinskas, "Equivalent circuit approach to the computer-aided analysis of switched capacitor circuits," *IEEE Trans. Circuits Syst.*, vol. CAS-26, pp. 708–714, Sept. 1979.

[8] J. Vandewalle, H. De Man and J. Rabaey, "The adjoint switched capacitor network and its applications," in *Proc. IEEE Symp. Circuits and Systems*, pp. 1031–1034, (Houston, TX), 1980.

[9] F. Brglez, "SCOP—A switched—capacitor optimization program," in *Proc. IEEE Symp. Circuits and Systems*, pp. 985–988, 1980.

[10] G. C. Fang and Y. P. Tsividis, "Modified nodal analysis with improved numerical methods for switched capacitive networks," in *Proc. IEEE Symp. Circuits and Systems*, pp. 977–980 (Houston, TX), 1980.

[11] H. De Man, J. Rabaey, G. Arnout, and J. Vandewalle, "DIANA as a mixed mode simulator for MOSLSI sampled—data circuits," in *Proc. IEEE Symp. Circuits and Systems*, pp. 435–438, (Houston, TX), 1980.

✚



Joos Vandewalle (S'71–M'77) was born in Kortrijk, Belgium, on August 31, 1948. He received the E. E. degree and the Ph.D. degree in applied sciences from the Katholieke Universiteit Leuven, Heverlee, Belgium, in 1971 and 1976, respectively.

From 1972 to 1976 he was Assistant at the E.S.A.T. Laboratory, Katholieke Universiteit Leuven. From 1976 to 1978 he was a Research Associate and from July 1978 to July 1979 he was Visiting Assistant Professor at the University of California, Berkeley. Since July 1979 he is back with the E.S.A.T. Laboratory of the Katholieke Universiteit Leuven, where he is Assistant Professor. His research interests are mainly in mathematical system theory and its applications in circuit theory and control.

✚



Hugo J. De Man was born in Boom, Belgium, on September 19, 1940. He received the electrical engineering degree and the Ph.D. degree in applied science from the Katholieke Universiteit Leuven, Heverlee, Belgium, in 1964 and 1968, respectively.

In 1968 he became a member of the staff of the Laboratory for Physics and Electronics of Semiconductors at the University of Leuven, working on integrated circuit technology. From 1969 to 1971 he was at the Electronic Research Laboratory, University of California, Berkeley, as an ESRO–NASA Post Doctoral Research Fellow, working on computer-aided device and circuit design. In 1971 he returned to the University of Leuven as a Research Associate of the NFWO (Belgian National Science Foundation). In 1974 he became a Professor at the University of Leuven. During the winter quarter of 1974–1975 he was a Visiting Associate Professor at the University of California, Berkeley. His actual field of research is the design of integrated circuits and computer-aided design.

✚



Jan Rabaey was born in Veurne, Belgium, on August 15, 1955. He received the E.E. degree from the Katholieke Universiteit Leuven, Heverlee, Belgium, in 1978. He is working towards the Ph.D. degree on the theory and application of switched capacitor filters in high quality audio systems.

In 1978 he obtained an I.W.O.N.L. fellowship which allows him to work as a Research Assistant at the Laboratory E.S.A.T., Katholieke Universiteit Leuven. In 1980, he obtained a fellowship as N.F.W. O.-aspirant.